Comparison of DC-Value Method and Kramers–Kronig Receiver in Optical OFDM SSB-DD Transmission

Yixian Dong, Romil K. Patel, Xiong Deng, *Member, IEEE*, A. N. Pinto, *Senior Member, IEEE*, Anlin Yi, Lin Jiang, *Member, IEEE*, Hui Yang, Xihua Zou, *Senior Member, IEEE*, Lianshan Yan, and Wei Pan

***Abstract*—Short reach optical communications are desperate for cost-effective solutions to improve capacity and compatibility in dealing with massive access and applications. Single sideband-direct detection (SSB-DD) is highly recognized for improving capacity with single PD, but it is confronted with signal-signal beating interference (SSBI). Recently, a DC-Value method has been proposed for optical signal phase retrieval for single carrier signal transmission. To further explore the effectiveness and compatibility of DC-Value method, in this letter for the first time, the orthogonal frequency division multiplexing (OFDM)-based multi-carrier modulation formats are processed by the DC-Value method in the receiver. Simulation results demonstrate that, for both OFDM and Nyquist-shaped single carrier (SC), the DC-Value method is beneficial in applying lower sampling rate to achieve comparable transmission performance than that of Kramers-Kronig receiver. In addition, although OFDM holds 2 dB increment of the optimum carrier-signal power ratio (CSPR) than Nyquist-SC, it offers more robustness to fibre transmission.**

***Index Terms*—Kramers-Kronig, DC-value method, OFDM, Nyquist single carrier.**

I. Introduction

SHORT reach optical communications within a distance of ∼100 km have been extensively investigated in both academic and industrial communities [1]. On one hand, the data centre interconnect (DCI) is upgrading the throughput towards to 400 Gbps or above while extending reach from 40 km to 80 km [1], [2]. On the other hand, the passive optical network (PON)-based optical and mobile converged network is in great demand of data rates and high compatibility [3], with good backward compatibility to existing 4 G networks using orthogonal frequency division multiplexing (OFDM). All the abovementioned applications in short reach links are desperate for cost-effective transceivers supporting high transmission capacity and good compatibility to deal with massive access and various applications [4]–[6].

For cost-effectiveness, intensity modulation and direct detection (IMDD) has been utilized for decades in short reach transmissions [2]. However, the chromatic dispersion (CD) in IMDD system has become a main factor preventing the transmission capacity improvement. Although coherent transceivers can provide more capacity and lower value of receiver sensitivity, its extremely high cost, complexity and energy consumption are not favorable in short reach links. To leverage the advantages of both IMDD and coherent transceivers, simplified self-coherent receivers have been widely explored [7], [8]. As one major method of self-coherent detection, the single sideband modulation and direct detection (SSB-DD) [9] can improve the optical spectral efficiency (SE) by either removing one of the two signal sideband, or transmitted different information bits in each sideband. In addition, a SSB-DD system can overcome the dispersion-induced power fading phenomena, gaining better SE and improving the fibre transmission distance. However, SSB-DD system suffers from the signal-signal beat interference (SSBI), which results from the nonlinear distortion intrinsic to the square-law detection of optical SSB (OSSB) signals.

Recently, a DC-Value method [10] has been proposed for reconstructing the optical signal phase using direct detection. It not only overcomes the signal-signal beat interference (SSBI) of SSB-DD system, but also greatly decreases the sampling rate compared to the Kramers-Kronig (KK) receiver [11]. In general, the nonlinear operations in the KK algorithm demand the DSP to be operated much faster than Nyquist sampling rate to accommodate spectral broadening effect [12]. The proposed DC-Value method imposes the minimum phase condition (MPC) [13] iteratively in the frequency domain without nonlinear operations, thus ensuring upsampling free reconstruction process. Another iterative method to mitigate the SSBI is the iteration SSBI cancellation algorithm [14]–[16]. This method works by calculating SSBI terms and subtracting them from the detected signal. However, due to the inaccuracy of the

Manuscript received 23 June 2022; revised 11 July 2022; accepted 15 July 2022. Date of publication 19 July 2022; date of current version 29 July 2022. This work was supported in part by China National Key R&D Programmes under Grants 2019YFB1803500, 2021YFB2800305, and 2021YFB2800801, in part by the National Natural Science Foundation of China under Grants 62001174 and 62101465, and in part by the Fundamental Research Funds for Central Universities under Grants 2682021CX041, 2682021CX043, and 2682021CG009. (*Corresponding author: Yixian Dong.*)

Yixian Dong, Xiong Deng, Anlin Yi, Lin Jiang, Hui Yang, Xihua Zou, Lianshan Yan, and Wei Pan are with the Center for Information Photonics and Communications, Southwest Jiaotong University, Chengdu 610031, China (e-mail: ydong@swjtu.edu.cn; xiongdeng@swjtu.edu.cn; anlinyi@swjtu.edu.cn; linjiang@swjtu.edu.cn; yanghuifly@home.swjtu.edu.cn; zouxihua@swjtu.edu.cn; lsyan@home.swjtu.edu.cn; wpan@swjtu.edu.cn).

Romil K. Patel and A. N. Pinto are with the Department of Electronics, Telecommunications and Informatics, University of Aveiro, 3810-193 Aveiro, Portugal (e-mail: romilkumar@ua.pt; anp@ua.pt).

Digital Object Identifier 10.1109/JPHOT.2022.3192263

SSBI approximation caused by the introduction of additional distortion by the linear filters, this technique has the drawback of limited effectiveness.

The DC-Value method with reduced sampling rate shows great advantages of transmission performance and implementation complexity in short haul transmissions [11], [17], [18]. However, the DC-Value method has only been investigated in the single carrier signal transmission. Short reach networks, including converged optical and wireless networks, are desperate for high compatibility to various modulation formats, such as multi-carrier based OFDM. To confirm the effectiveness of the DC-Value method in OFDM signal transmission, the corresponding characteristics are intensively investigated and compared with the single carrier transmission. The main contributions of this paper can be summarized as follows:

- With different intrinsic peak-to-average power ratios (PAPR) in single carrier and multi-carrier formats, the optimum carrier-signal power ratios (CSPR) are compared via different optical signal to noise ratios (OSNR) and fibre transmission distances. The comparison between OFDM and Nyquist-SC shows that OFDM system requires higher optimum CSPR, but demonstrating better performance within the larger OSNR range and more robust to fibre CD.
- To explore the effectiveness of DC-Value method, different sampling rates are applied in the SSB-DD system. It is shown that Nyquist sampling rate is enough for the DC-Value method to recover the phase of OFDM and Nyquist-SC signal, resulting nearly half decrement of arithmetic operations than that of KK receiver.
- Different modulation orders for quadrature amplitude modulation (QAM) in OFDM and single-carrier signalling are analysed and their transmission performance under various OSNR condition are explored, confirming the effectiveness of the DC-Value method.
- The DC value estimation is further investigated in OFDM systems. The analysis and simulations show that the DC estimation within a $\pm 5\%$ error can fully exploit the advantages of the DC-Value method.

The remainder of this paper is organized as follows. In Section II, we describe the model of a general SSB-DD system with conventional KK receiver and DC-Value method applying OFDM and Nyquist-SC, respectively. The DC estimation method in practice is also introduced. In Sections III, simulation results are presented and discussed in aspects of optimum CSPR, OSNR effect, transmission distance, PAPR and implementation complexity. Finally, the effectiveness of the DC estimation method is verified. Section IV draws conclusions from this paper.

II. System Model

The schematic diagram of the SSB-DD system is depicted in Fig. 1. There are various ways to produce OSSB signal, and in this letter the virtual digital carrier-assisted method [19] is considered for the consistent transmission condition in the previous publication [10], [18]. Furthermore, this method can balance the performance and implementation cost, and it also offers precise

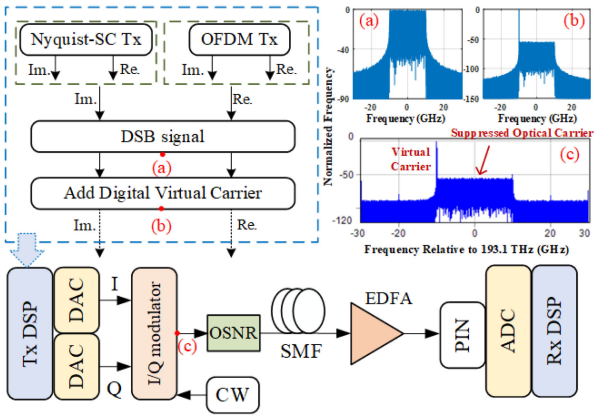

Fig. 1. Schematic of the SSB-DD transmission system.

dynamic CSPR adjustment and utilizes the full bandwidth of the DAC. Other OSSB signal generation methods, such as coupling an additional laser source as the optical carrier, can be further investigated in future works. In the Tx DSP, the generated digital OFDM/Nyquist SC signals, at point (a), are firstly added by a digital carrier, producing a digital carrier-assisted SSB signal (point (b)). Then the signals are sampled within 2 DACs. To generate the OSSB signal, the IQ modulator in biased at the null-point to suppress the optical carrier, which is shown in Fig. 1(c). For the self-coherent detection within a single PD, normally a strong optical tone from an additional laser source or a comb generator is required, which significantly increases the implementation cost. While the digitally-generated tone acts as a virtual carrier for self-coherent detection. The virtual carrier assisted OSSB signal at point (c) in Fig. 1, can be written as

$$[E(t) = \left[s(t) + Ae^{-j\left(2\pi\frac{B}{2}t+\Phi\right)}\right] e^{-j\omega_c t}, \tag{1}$$

where A is the optical tone's amplitude, $s(t)$ is the transmitted signal, B is the bandwidth of the information-bearing signal, and ω_c refers to the optical carrier central frequency with the phase of Φ. After fibre transmission, the received signal is fed into a single PD, followed by the ADC to sample the signal into Rx DSP block for further signal processing. The detected signal fed into the Rx DSP can be written as:

$$I(t) = |E(t)|^2 = |A|^2 + 2\mathrm{Re}\left\{A^* e^{-j\left(2\pi\frac{B}{2}t+\Phi\right)} s(t)\right\} + |s(t)|^2, \tag{2}$$

where the first term is the DC component, the second term is the information-bearing signal, and the last term is signal-signal beat interference (SSBI) component which falls in-band and causes performance degradation.

In Fig. 2, the Rx DSP blocks present the conventional KK receiver (Fig. 2(c)) and DC-Value method (Fig. 2(d)) to recover the phase of OFDM (Fig. 2(a)) and Nyquist-SC (Fig. 2(b)) signal, respectively. For the KK receiver, the Nyquist SC and OFDM signals are recovered simply using the KK relation, as shown in Fig. 2(c) where the conventional KK schematic diagram is presented with oversampling and downsampling. In the DC-Value method of Fig. 2(d), a square-root operation is firstly carried out to obtain the magnitude of the optical

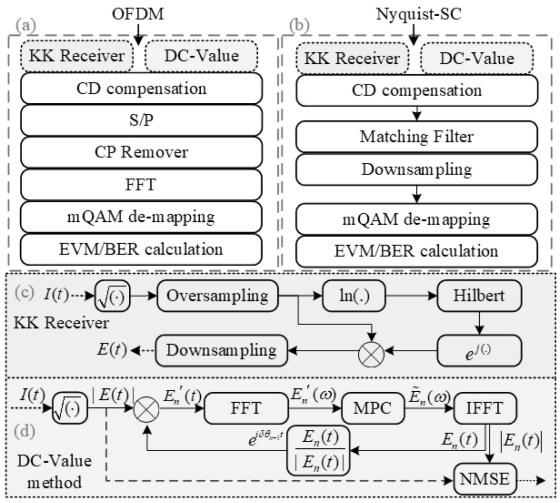

Fig. 2. DSP block of (a) Nyquist-SC; (b) OFDM; (c) KK receiver; (d)DC-Value method.

field, followed by the multiplication with the phase correction factor $e^{i\delta\theta_{n-1}t}$, to generate the complex signal $E'_n(t)$. In the first iteration ($n = 1$), the phase correction vector is assumed to be zero, i.e. $\delta\theta_0 = 0$. Next, the MPC is imposed on the Fourier transformed signal $E'_n(\omega)$ to attain $\tilde{E}_n(\omega)$ by:

$$\tilde{E}_n(\omega) = \begin{cases} p\tilde{E'}_n(\omega), & \text{for}\omega > 0 \\ NE_o, & \text{for}\omega = 0 \\ 0, & \text{for}\omega < 0 \end{cases}, \tag{3}$$

where $p = 2$ if $n = 1$, otherwise, $p = 1$. After imposing MPC, the IFFT of the $\tilde{E}_n(\omega)$ is computed to obtain the first estimate of the minimum phase signal $E_1(t)$. The phase correction vector corresponds to $E_1(t)$ can be calculated. This phase estimation is then supplied as an updated phase correction vector for the subsequent iteration ($n = 2$). Here the normalized mean squared error (NMSE) between the known magnitude $|E(t)|$ and the estimated magnitude $|E_n(t)|$ is calculated, which is monotonically decreasing after each iteration and has a lower bound to be zero. Ideally, when $n \to \infty$, the reconstructed signal can be infinitely close to minimum phase signal, and the erroneous mismatch can be negligible.Therefore, the reconstruction process converges. Afterwards, the reconstructed minimum phase signal $E_n(t)$ is passed through the DC remover and then shifted to the baseband.

For the receiver utilizing an alternating current (AC) coupled PD, the effectiveness of both KK receiver and DC-Value method are highly dependent on the estimated DC value, which, however, is not available at the input of the subsequent DSP block. A couple of methods have been proposed to estimate this DC value. The method proposed for single carrier in [18] does not require preamble as in [20], neither need multiple interactions as in [11]. To explore its effectiveness and characteristics for OFDM signal, this DC value estimation method is utilized in this letter. The amplitude of DC value is approximated by

$$DC \approx \left[\left\langle \mathrm{I_{AC}}^2(\mathrm{t})\right\rangle \frac{CSPR}{2}\right]^{1/4}, \tag{4}$$

and its effects on transmission performance are presented in Section III.

III. Performance Comparison

In this section, we evaluate and compare the performance of conventional KK receiver and DC-Value method applied in SSB-DD system for both Nyquist-SC and OFDM modulation formats. For fair comparisons, both Nyquist-SC and OFDM signal are utilized with 16-QAM. In particular, OFDM signal are transmitted with 128 subcarriers and its cyclic prefix is set to be 0 as chromatic dispersion compensation is applied in the Rx DSP. The real and imaginary parts of the complex signal are both sampled at Nyquist sampling rate of 20 GS/s in the transmitter DSP. Here we define the oversampling factor R is the ratio of the sampling rate in the DSP block divided by the Nyquist sampling rate (i.e., twice the bandwidth of the signal). Thus when the system is sampled at one (two) Nyquist sampling rate, the oversampling factor $R = 1$ (2). In Nyquist-SC case, the complex signal are generated using a square root raised cosine (SRRC) pulse shaping filter with the roll-off factor = 0, so that its spectral width is comparable with that of the OFDM signal. Therefore, the single carrier and multi-carrier transmission are under the similar transmission condition, confirming the fairness and effectiveness of the comparison. In Fig. 1(a), the spectrum of the generated double side band (DSB) Nyquist-SC signal when $R = 2$ is presented. After adding the digital carrier or a DC value, the corresponding spectrum is inserted in Fig. 1(b). The generated virtual carrier-assisted OSSB signal is at optical central frequency of 1550 nm with no guardband between the carrier and signal. Other parameters in our simulations are listed in the Table I if not otherwise specified. It is worthy noting that in this section, the system OSNR is set to be 35 dB, which is large enough to reduce the noise affecting the transmission system to have a valid comparison between the two methods. And the iteration number of 10 is utilized in the DC-Value method for precise estimation and comparison. Normally, an iteration number of 5 is enough for signal phase retrieval [18], which will be explained in the following part.

A. The Optimum CSPR

In SSB-DD system, the CSPR is the key parameter to determine the transmission performance [10]. A large CSPR value can guarantee the MPC for precise signal phase recovery. While for a fixed optical launch power, the larger the CSPR implemented, the less the signal power imposed, thus the decreased signal-to-noise ratio (SNR) degrades the transmission performance. To explore the optimum CSPR in Nyquist-SC and OFDM system, the optical back to back (OB2B) transmission system are investigated with oversampling factor $R = 1$ and $R = 2$ in Fig. 3, by its error vector magnitude (EVM) variation. Fig. 3(a) shows that, when $R = 1$, for both Nyquist-SC and OFDM, the performance

TABLE I
POWER ALLOCATION STRATEGY

Parameter	Value	Parameter	Value
Nyquist Sampling Rate	20 GS/s	Oversampling Rate R	1, 2
OSNR	35 dB	CW operation wavelength	1550 nm
Clipping ratio	14 dB	ENOB (effective NO. of bits)	8 bit
Optical launch power	1 mW	Received optical power	0 dBm
Standard single mode fibre (SSMF) attenuation	0.2 dB/km	SSMF nonlinear parameter	2.6×10^{-20} m^2/W
SSMF dispersion	16×10^{-6} s/m^2	SSMF dispersion slope	0.08×10^{3} s/m^3
PD noise current spectral density	10 $pA/\sqrt{Hz}$)	DC-Value method iteration number	10

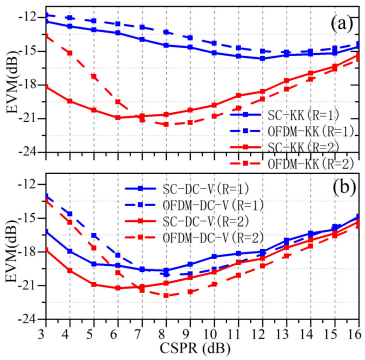

Fig. 3. EVM vs CSPR of (a) KK receiver (b) DC-Value method.

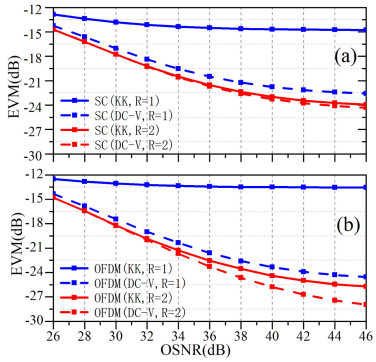

Fig. 4. EVM vs OSNR of (a) Nyquist-SC; (b) OFDM.

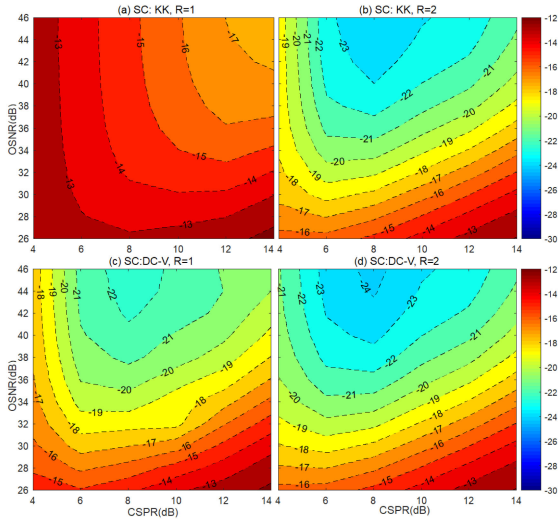

Fig. 5. EVM contour of Nyquist-SC: OSNR vs CSPR of (a) R = 1:KK receiver; (b) R = 2:KK receiver; (c) R = 1: DC-Value method; (d) R = 2: DC-Value method.

of conventional KK receiver are highly limited over all the CSPR value range, due to the spectral broadening caused by nonlinear operations [12]. While the DC-Value method can achieve EVM below -17 dB (corresponding to BER of 1×10^{-3}) within the CSPR range between 5 dB and 13 dB, when $R = 1$ as shown in Fig. 3(b). Such reduction of sampling rate can greatly cut down the implementation complexity and cost in practice. When $R = 2$, the spectrum broadening-induced signal distortion is not the dominating factor affecting the transmission performance. Thus, the KK receiver and DC-Value method achieve similar performance for each modulation format.

Meanwhile, it is noted that the optimum CSPR for the lowest EVM of single carrier and OFDM are obtained at 6 dB and 8 dB, respectively. The 2 dB CSPR increment of OFDM signal is a result of its higher PAPR than single carrier. A large PAPR tends to violate the MPC for a given CSPR, thus the optimum CSPR is increased. The crossing point of the EVM curves for single carrier and OFDM are obtained around 7 dB, indicating the similar MPC and noise power.

B. OSNR and CSPR on EVM

To investigate the effect of OSNR, Fig. 4 shows the EVM varies with the OSNR while fixing the CSPR at 8 dB for both Nyquist-SC and OFDM. It can be seen that in the higher OSNR range when $R = 2$, the DC-Value method outperforms the KK receiver for OFDM signal, while for Nyquist-SC case, both methods have similar trend. This is due to the fact that the OFDM system meets the optimum MPC at CSPR of 8 dB, and OSNR values play a key role in determining the transmission performance. While for Nyquist-SC signal at CSPR of 8 dB, the noise is a dominating factor of determining the performance, thus, with the same OSNR, both KK and DC-Value method has similar EVM.

To further confirm above observations and have an overview on effects of OSNR and CSPR, the EVM contour versus OSNR and CSPR are presented in Fig. 5 and Fig. 6, for Nyquist-SC and OFDM signal, respectively. It is clear that, with the same CSPR value, higher OSNR results in better transmission performance. When the OSNR is lower than 28 dB and the CSPR is lower than 8 dB, the EVM of Nyquist-SC can reach below -17 dB,

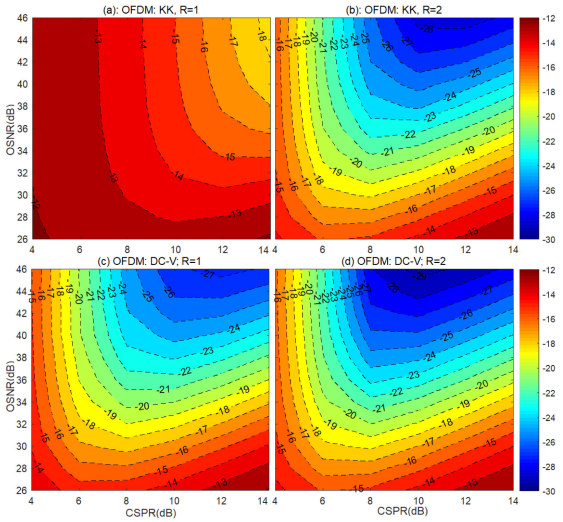

Fig. 6. EVM contour of OFDM: OSNR vs CSPR of (a) R = 1:KK receiver; (b) R = 2: KK receiver; (c) R = 1: DC-Value method; (d) R = 2: DC-Value method.

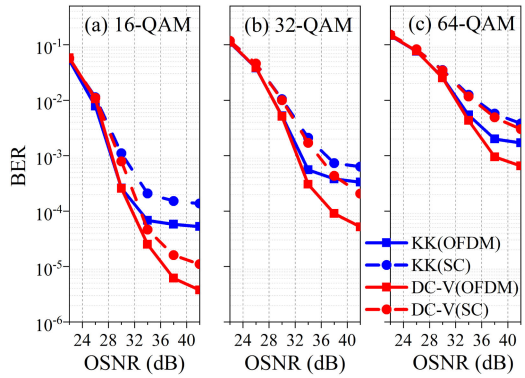

Fig. 7. BER vs OSNR of (a) 16-QAM; (b) 32-QAM; (c) 64-QAM.

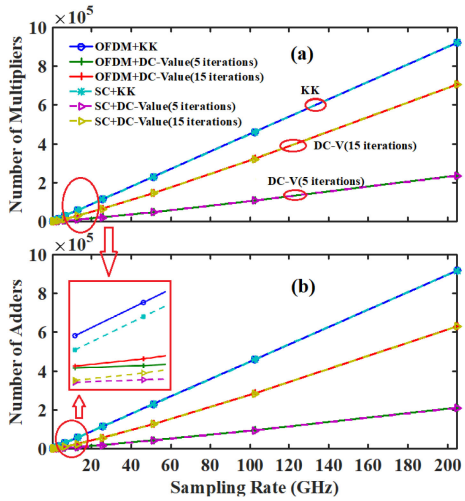

Fig. 8. (a) Number of multipliers; (b) Number of adders.

while system with OFDM signal can only work with higher OSNR and CSPR value. Comparing the Fig. 5(b) and Fig. 6(b) when OSNR = 36 dB, at CSPR = 6 dB, the single carrier shows better performance as EVM >21 dB can be obtained in KK receiver of $R = 2$, while OFDM case can only reach EVM <20 dB. While increasing CSPR to 12 dB, OFDM performs better than that of a single carrier because of its higher optimum CSPR value. It also can be seen that over the range of OSNR below 36 dB, the Nyquist-SC and OFDM signal obtain the optimum CSPR at 6 dB and 8 dB respectively. When OSNR is above 36 dB, both modulation formats shift their corresponding optimum CSPR range to higher range, due to decreased noise power.

In addition, the achievable EVM of OFDM can be further improved as darker color are presented within higher OSNR range in Fig. 6(b)–(d), than that of Nyquist-SC in Fig. 5(b)–(d). Particularly, the similarity of EVM contour between the DC-Value method of $R = 1$ and KK receiver of $R = 2$, indicates that the comparable transmission performance of these two methods can be obtained with both OFDM and Nyquist-SC cases. It shows that over a wide range of OSNR and CSPR values, the DC-Value method can apply half sampling speed than conventional KK receiver, significantly reducing complexity and power consumption.

Besides 16-QAM, higher modulation formats such as 32-QAM and 64-QAM are applied in the this SSB-DD system, utilizing the CSPR at 8 dB and the oversampling rate R of 2. From Fig. 7, it can be seen that when OSNR is in the larger value range, the DC-Value method are superior than conventional KK method for various orders of QAM modulation format. To reach the BER of 1×10^{-3} by the DC-Value method, the required OSNR of OFDM signal with 16-QAM, 32-QAM and 64-QAM are 28 dB, 33 dB, 38 dB, respectively. When increasing the order of QAM modulation formats, the optimum CSPR is also increased [10]. Thus, the applied 8 dB-CSPR deviates from the optimum value of 32-QAM/64-QAM signals, further deteriorating their transmission performance.

C. DSP Hardware Complexity

For system achieving comparable performance by DC-Value method of $R = 1$ and KK method of $R = 2$, their Rx DSP hardware implementation complexity are presented in Fig. 8 for both OFDM and Nyquist-SC. Here considering a DSP chip with clock frequency $f_{clock} = 200$ MHz, parallelization of N is employed to realize a high sampling frequency by $N = \lceil f_s / f_{clock} \rceil$, where $\lceil \cdot \rceil$ is the ceiling operator. The KK method requires digital signal upsampling and downsampling, which can be realized by an FIR filter with $N_s = 128$ taps. The Hilbert transformation in the KK method can be implemented using an FIR filter having $N_h = 128$ taps. The corresponding number of adders and multipliers are listed in Table II. The OFDM signal with 128 subcarriers adding a fixed multipliers of $\frac{L}{2} \cdot \log 2(L)$ and adders of $L \cdot \log 2(L)$, with FFT size $L = 128$. While Nyquist-SC increases the multipliers by including SRRC shaping and matching filters, here $N_{taps} = 128$ is also considered. Varying the iteration number k of 5 and 15 in DC-Value method, the implementation multipliers and adders versus the sampling rate

TABLE II
HARDWARE COMPLEXITY COMPARISON

	conventional KK receiver	DC-Value method	OFDM	Nyquist-SC
Number of adders	$(3N_s + N_h/2)RN$	$(4N\log_2 N + N)k$	$L \cdot \log 2(L)$	N_{taps}
Number of multipliers	$(3N_s + N_h/2 + 2)RN$	$(4N\log_2 N + 6N)k$	$\frac{L}{2} \cdot \log 2(L)$	N_{taps}

N_s: FIR filter taps for KK upsampling/downsampling, N_h: FIR filter taps for KK Hilbert transformation, R: oversampling rate, N: parallelization number for high sampling frequency. k: iteration number, L: FFT size of OFDM, N_{taps}: SRRC filter taps.

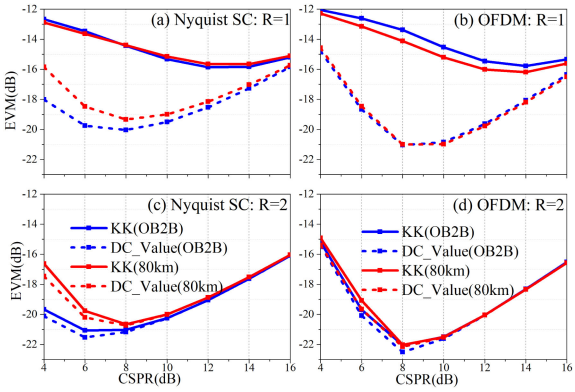

Fig. 9. EVM vs CSPR in OB2B and 80 km SSMF transmission: (a) R = 1:Nyquist SC; (b) R = 1: OFDM; (c) R = 2:Nyquist SC; (d) R = 2: OFDM.

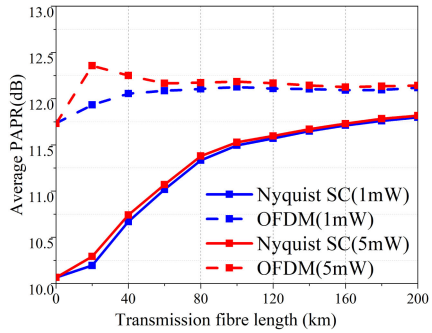

Fig. 10. Average PAPR of OFDM and Nyquist SC.

are calculated in Fig. 8(a)(b). It can be seen that, comparing to the conventional KK receiver, the DC-Value method can decrease the number of adder and multipliers significantly even for a large iteration number of 15. This is because the oversampling factor R is the dominating factor determining the overall number of arithmetic operations. In the inserted and enlarged figure, the number of adders for implementing OFDM signal contributes a bit more complexity than that of Nyquist-SC. However, such contribution is negligible over all Rx DSP complexity.

D. Fibre Transmission

From previous results, we know that the OFDM possessing higher PAPR requires higher optimum CSPR, however, it is shown to be more robust to the fibre transmission. In Fig. 9, transmission of 80 km over standard single mode fibre (SSMF) are compared with OB2B transmission for both modulation formats. The simulation results in Fig. 9(a)(c) show that for Nyquist-SC, after transmission of 80 km, the performance is degraded compared to OB2B in particular for lower CSPR range. In Fig. 9(c), the optimum CSPR is shifted from 6 dB to 8 dB by both methods. Because of the constructive and/or destructive superposition of successive signal pulses due to the chromatic dispersion (CD) [21], the PAPR of the Nyquist-SC increases with transmission fibre distance. Thus, its optimum CSPR is shifted to higher value after 80 km transmission. The average PAPR of Nyquist-SC after the photo-detection is calculated and shown in Fig. 10, where the solid curves show the average PAPR of single carrier is raised with the propagation distance, as a result of the chromatic dispersion accumulation with the fibre length.

Meanwhile, for the OFDM signal, the average PAPR (the dotted lines in Fig. 10) keeps flat along the propagation distance. This is due to the fact that the noise-like characteristics of the OFDM waveform can be well-approximated by a Gaussian process with the strictly band-limited power spectrum. The Gaussian approximation is still valid after experiencing the fiber dispersion. Thus, the performance after 80 km transmission is comparable to that of OB2B in Fig. 9(b)(d). Furthermore, there is PAPR enhancement around fibre length of 20∼40 km in Fig. 10, which is in agreement of [21]. This PAPR enhancement is caused by fiber nonlinearity and/or some interactions between the nonlinearity and the dispersion such as the higher order soliton compression or the modulation instability. This can be confirmed by the red dotted curve, which utilizing higher optical launch power at 5 mW. As the fibre nonlinearity is enhanced, the corresponding PAPR enhancement is also increased. With the increment of propagation distance, the accumulated chromatic dispersion becomes the dominating factor, thus the average PAPR reduces to a flat end. In all, the overall average PAPR of OFDM is larger than single carrier, confirming its higher optimum CSPR in previous sections.

E. DC Value Estimation of OFDM Signal

In this subsection, the effectiveness and characteristics of the DC vale estimation by (4) for OFDM signal reconstruction are investigated. The DC estimation benchmark is estimated by (4). When the DC value is applied with its benchmark, the corresponding constellations from iteration number 1 to 15 are presented in Fig. 11. It can be seen that after iteration of 5, the constellation points slightly changes, confirming the convergence of the iteration. For the DC-Value method with only 5 iterations, the signal processing time would not exceed several

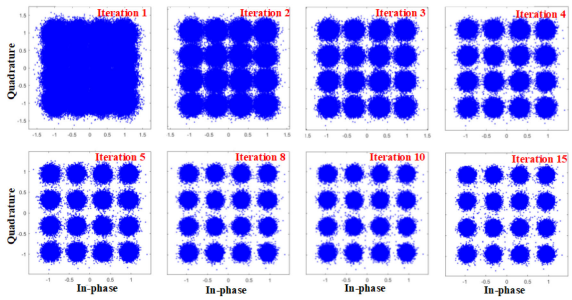

Fig. 11. Constellations after different iterations.

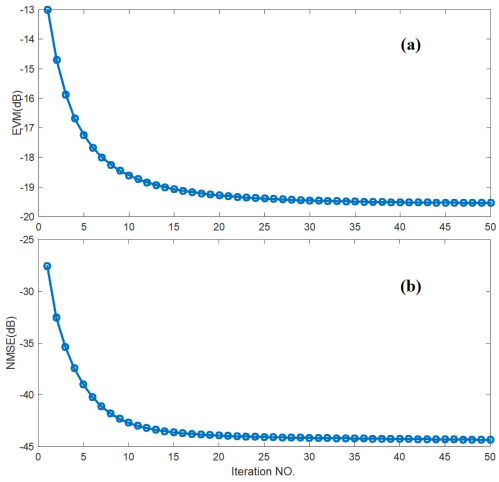

Fig. 12. DC-Value method for $R = 1$: (a) EVM vs iteration number; (b) NMSE vs iteration number.

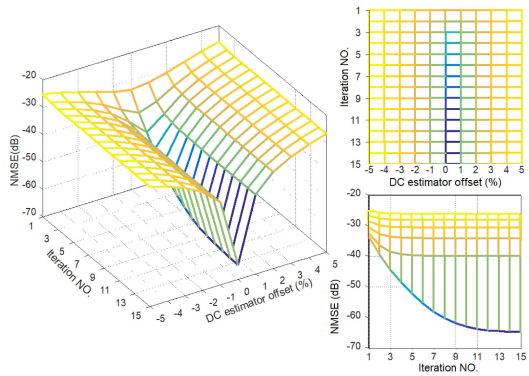

Fig. 13. NMSE of different DC estimation offset and iterations.

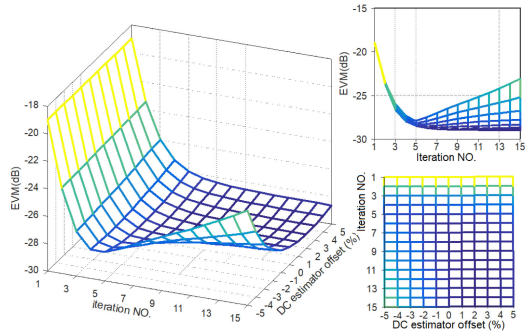

Fig. 14. EVM of different DC estimation offset and iterations.

microseconds, and such latency can be tolerated by the total end-to-end latency requirement for the high-speed transmission. To further confirm the stability and convergence of DC-Value method, the EVM and NMSE variations with $R = 1$ for enlarged iteration number 50 is presented in Fig. 12. It can be seen that the EVM and NMSE iterative values keep stable over iteration number 15 to 50. Moreover, these two curves tend to be flat if further increasing the iteration number. Thus, it indicates that the DC-Value method is stable with converged results.

To have an overview analysis of iteration number and DC estimation error, the 3D analysis of NMSE and EVM over 15 iterations while varying the DC estimation from its benchmark to $\pm 5\%$ offset are calculated in Fig. 13 and Fig. 14, respectively. It can be seen that for DC estimation offset $= 0\%$, the NMSE converges to below -50 dB after 5 iterations, confirming the effectiveness of DC-Value method. If the estimated DC value offset increases, the NMSE becomes nearly independent of the number of iterations, preventing a proper convergence of the DC-Value method, thus resulting in a limited reconstruction accuracy. For an estimation error greater than $\pm 3\%$, a 20 dB NMSE penalty is observed in the numerical analysis after 5 iterations. Fig. 14 shows that an EVM threshold of -28 dB can be assured after 5 iterations if DC estimation error falls within approximately $\pm 5\%$ range. It is demonstrated that for OFDM signal, the DC estimation within a $\pm 5\%$ error can fully exploit the advantages of the DC-Value method.

It is also noted that, the results are asymmetric for the positive and negative offset errors with both NMSE and EVM. As the complex SSB signal requires a non-negative real part to satisfy the MPC, the positive offset value leads to a higher DC value so the real part of the signal becomes non-negative (with high CSPR). On the other hand, the negative offset causes a real part of the signal to approach a negative value and reduces the CSPR. Also, a very high negative offset can violate the MPC as well. Therefore, the signal reconstruction becomes more erroneous in the negative offset error.

IV. Conclusion

In this letter, we have presented a comprehensive analysis and comparisons for the SSB-DD system with the DC-Value method and conventional KK receiver utilizing both single carrier and multi-carrier modulation formats. Results have demonstrated that, the DC-Value method can achieve EVM below -17 dB over the range of CSPR from 5 dB to 13 dB at Nyquist sampling rate, while conventional KK receiver demanding at least doubled Nyquist sampling rate. Moreover, by comparing the arithmetic operations of these two methods, the DC-Value method has shown great advantages in decreasing complexity and cost than KK receiver. We have also found that Nyquist-SC signal has been proved work better than OFDM signal when the OSNR is lower than 28 dB and the CSPR is lower than 8 dB. In addition,

OFDM signal requires around 2 dB higher optimum CSPR value than that of single carrier, due to its high PAPR, but it has higher tolerance to fibre transmission. Finally, the DC value estimation method has been explored and its effectiveness is confirmed for OFDM signal.

REFERENCES

[1] X. Pang *et al.*, "High-speed short reach optical communications: Technological options and challenges," in *Proc. Asia Commun. Photon. Conf./Int. Conf. Inf. Photon. Opt. Commun.*, 2020, pp. 1–3.

[2] X. Zhou, R. Urata, and H. Liu, "Beyond 1 Tb/s intra-data center interconnect technology: IM-DD OR coherent?," *J. Lightw. Technol.*, vol. 38, no. 2, pp. 475–484, 2020.

[3] N. Suzuki, H. Miura, K. Mochizuki, and K. Matsuda, "Simplified digital coherent technologies for beyond 100G optical access systems in the B5G/6G era," in *Proc. Opt. Fiber Commun. Conf. Exhib.*, 2021, pp. 1–3.

[4] A. Tzanakaki, M. P. Anastasopoulos, and D. Simeonidou, "Converged optical, wireless, and data center network infrastructures for 5G services," *J. Opt. Commun. Netw.*, vol. 11, no. 2, pp. A111–A122, 2019.

[5] J. Zhang *et al.*, "The best modulation format for symmetrical single-wavelength 50-Gb/s PON at O-band: PAM, CAP or DMT?," in *Proc. Opt. Fiber Commun. Conf. Exhib.*, 2021, pp. 1–3.

[6] S. Sarmiento *et al.*, "High capacity converged passive optical network and RoF-based 5G fronthaul using 4-PAM and NOMA-CAP signals," *J. Lightw. Technol.*, vol. 39, no. 2, pp. 372–380, 2021.

[7] R. I. Killey, M. S. Erkilinç, W. Yi, and P. Bayvel, "Low complexity self-coherent transceivers for metro, access and inter-datacenter applications," in *Proc. Opt. Fiber Commun. Conf. Exhib.*, 2019, pp. 1–3.

[8] D. Milovančev, N. Vokić, F. Karinou, and B. Schrenk, "Simplified coherent receiver for zero-touch wireless integration in power-splitting ODN with >40 dB budget," in *Proc. Opt. Fiber Commun. Conf. Exhib.*, 2021, pp. 1–3.

[9] M. Sieben, J. Conradi, and D. Dodds, "Optical single sideband transmission at 10 Gb/s using only electrical dispersion compensation," *J. Lightw. Technol.*, vol. 17, no. 10, pp. 1742–1749, 1999.

[10] R. K. Patel, I. A. Alimi, N. J. Muga, and A. N. Pinto, "Optical signal phase retrieval with low complexity DC-value method," *J. Lightw. Technol.*, vol. 38, no. 16, pp. 4205–4212, Aug. 2020.

[11] A. Mecozzi, C. Antonelli, and M. Shtaif, "Kramers–Kronig receivers," *Adv. Opt. Photon.*, vol. 11, no. 3, pp. 480–517, Sep. 2019.

[12] T. Bo and H. Kim, "Toward practical Kramers-Kronig receiver: Resampling, performance, and implementation," *J. Lightw. Technol.*, vol. 37, no. 2, pp. 461–469, Jan. 2019.

[13] T. Wang and A. J. Lowery, "Minimum phase conditions in Kramers-Kronig optical receivers," *J. Lightw. Technol.*, vol. 38, no. 22, pp. 6214–6220, Nov. 2020.

[14] Z. Li *et al.*, "SSBI mitigation and the Kramers–Kronig scheme in single-sideband direct-detection transmission with receiver-based electronic dispersion compensation," *J. Lightw. Technol.*, vol. 35, no. 10, pp. 1887–1893, 2017.

[15] C. Sun, D. Che, H. Ji, and W. Shieh, "Investigation of single-and multi-carrier modulation formats for Kramers–Kronig and SSBI iterative cancellation receivers," *Opt. Lett.*, vol. 44, no. 7, pp. 1785–1788, 2019.

[16] C. Sun, D. Che, H. Ji, and W. Shieh, "Study of chromatic dispersion impacts on Kramers–Kronig and SSBI iterative cancellation receiver," *IEEE Photon. Technol. Lett.*, vol. 31, no. 4, pp. 303–306, Feb. 2019.

[17] R. K. Patel *et al.*, "Virtual carrier assisted self-coherent detection employing DC-value method," in *Proc. Opt. Fiber Commun. Conf. Exhib.*, 2021, pp. 4–6.

[18] R. K. Patel *et al.*, "Impact of the carrier contribution factor in the self-coherent DC-value method," *Opt. Exp.*, vol. 29, no. 25, pp. 41234–41 245, 2021.

[19] W.-R. Peng *et al.*, "Experimental demonstration of a coherently modulated and directly detected optical OFDM system using an RF-tone insertion," in *Proc. Conf. Opt. Fiber Commun./Nat. Fiber Optic Eng. Conf.*, 2008, pp. 1–3.

[20] T. Bo and H. Kim, "DC component recovery in Kramers–Kronig receiver utilizing AC-coupled photo-detector," *J. Lightw. Technol.*, vol. 38, no. 16, pp. 4307–4314, 2020.

[21] Y. Yoshida, A. Maruta, and K.-I. Kitayama, "On the peak-to-average power ratio distribution along fiber in the optical OFDM transmissions," in *Proc. 37th Eur. Conf. Expo. Opt. Commun.*, 2011, pp. 1–3.